15

Video-enhanced Microscopy Investigation of Emulsion Droplets and Size Distributions

Øystein Sæther
Norwegian University of Science and Technology, Trondheim, Norway

I. INTRODUCTION

Video-enhanced microscopy (VEM, or video micro-scopy, VM) is a technique that combines the magnification power of a microscope with the imageacquisition capability of a video camera. The resulting data matrix, from which information about the sample can be extracted, is an image or a series of images. This intimately relates VM to image-analysis techniques, now frequently with the assistance of a computer. Current image-analysis software provides a wide range of analytical features, in addition to image enhancement (the improvement of image quality prior to analysis), which is only briefly treated here. It is obvious that image analysis is not restricted to VM, but finds application within any technique where the data take the form of an image, e.g., electron microscopy, and other video or photographic techniques.

Typical information that can be found in images is sample state, geometry, dispersity, etc. For emulsions, this generally means droplet size and concentration, which are important properties of any emulsion. Figure 1 shows a coarse and a fine emulsion, the behavior of which can be expected to differ strongly due to droplet size and concentration. Further, the state of fiocculation will indicate droplet/droplet interactions. Series of images or continuous video provide information about droplet interactions and the kinetics of important processes within the emulsion, like fiocculation and coalescence. All the above parameters are central to the understanding of emulsion behavior and emulsion stability.

Microscopy (1-5), photomicrography (6-28), and VM (29-49) have combined a long history in the determination of particle and droplet size. A number of studies have been performed comparing the microscopy methods to alternative methods, such as those of light scattering (10, 32, 50), Coulter counting (2, 5, 24, 32, 50), turbidimetry (3, 9, 27), NMR (33, 45, 46), and others (8, 15, 28). Generally, the comparison is favorable and objections often relate to the labor-intensity of the derived methods. Amongst many applications reported in the literature are the study of vesicles (size and shape) (51, 52), particle trajectories (53) and emulsion (suspension) kinetics (26, 38, 41, 48, 54-61), measurement of pair potentials (62), film studies and interfacial tension measurements (63-68), and emulsions in electric fields (3, 13, 69, 70) (Fig. 2), to name but a few, to illustrate the versatility of such techniques.

II. CHARACTERISTICS OF THE TECHNIQUE

Figure 3 shows a schematic of a typical VEM set-up. A video camera (digital or analog) is attached to the phototube

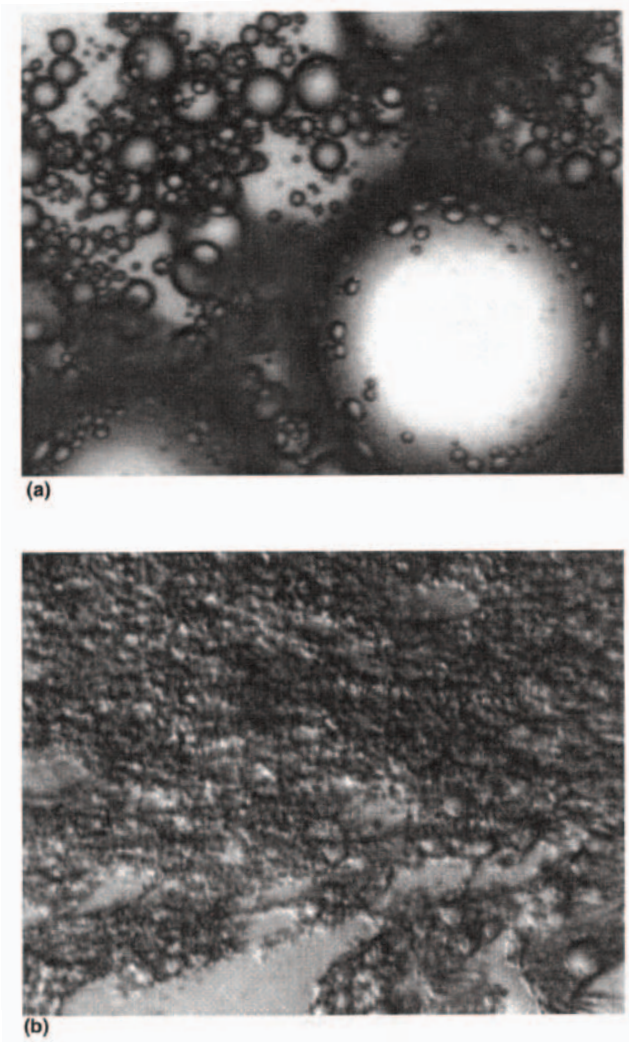

Figure 1 (a) Emulsion mixed with a simple rotor paddle; the uneven distribution of mechanical energy on the liquids has caused a broad DSD. (b) Ultrasonically prepared emulsion; the dispersed volume is to a high degree present as very small droplets in a narrowly distributed fraction of the population.

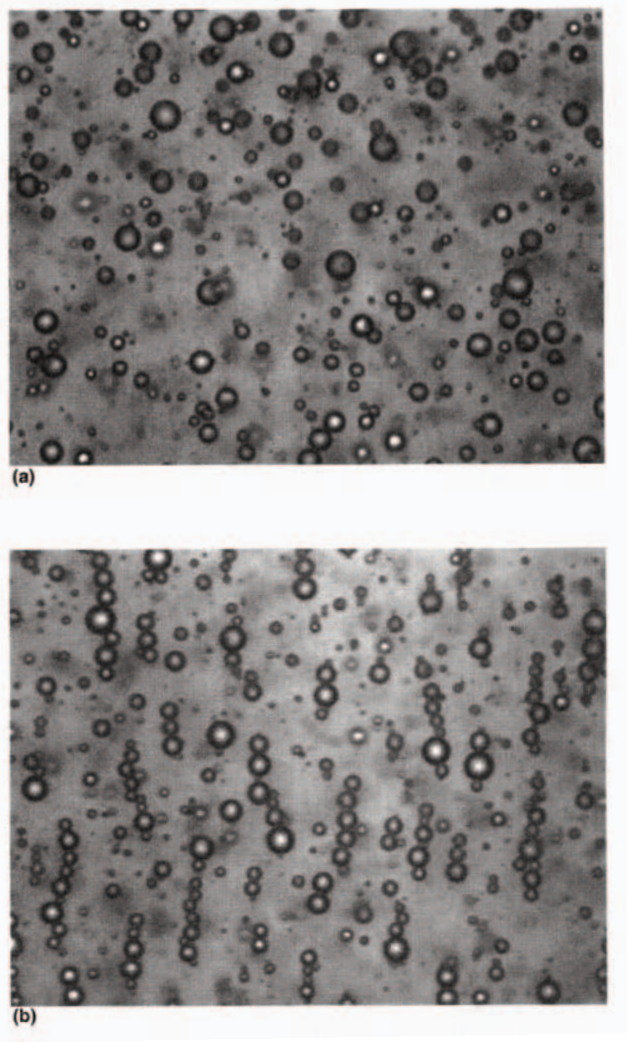

Figure 2 Aqueous droplets dispersed in crude oil and sub-jected to an electric field: (a) no field; (b) 5 s, 1 kV/cm -droplet orientation in chains along the direction of the field. The droplets become small net dipoles in the dielectric oil continuum and are attracted to each other, forming chains in the direction of the field. High field strengths will cause interdroplet membrane rupture and coalescence. The principle has been utilized for measuring emulsion stability (i.e., resistance to electrically forced breakdown) in the high voltage-time domain spectroscopy (HiV-TDS) (71,72) and conductivity techniques (73).

of a microscope. The image is transferred to the image captureboard installed on to the computer motherboard (digitization). Image enhancement and analysis is accomplished with image-analysis software.

Careful adjustment of the microscope is essential for the achievement of reliable and reproducible results. Light-source intensity, the focussing of optics, and the adjustment of field and condenser diaphragms must be carefully controlled. As the droplets are defined by their circumference gray tone (or color) levels, deviations in the above from image to image may cause differing measurements of equally sized droplets. Also, it is important to realize the operational characteristics of the components in the system. For example, the video camera is a vital link in the chain, and different models will handle the relay of the microscope image differently. For CCD cameras, an important property is the pixel geometry - some cameras have square, others rectangular, pixels, influencing the data matrix forwarded to the captureboard.

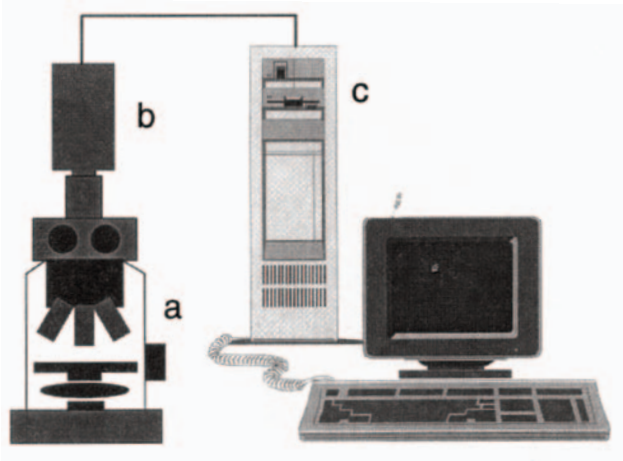

Figure 3 Main components of the VEM experimental setup: (a) the microscope, including optics; (b) the video-camera; (c) the computer with captureboard and image-analysis software.

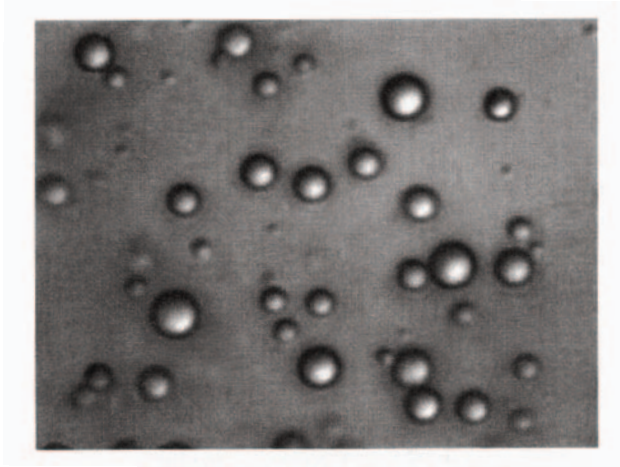

Figure 4 DIC image of O/W emulsion. The droplets appear in relief; droplets beyond the infocus section appear blurred.

Tremendous advances in the development of microscope optical components (fiters, objectives) have gradually increased the range of applications for microscopy, especially by improving contrast between the objects of interest and the background. Much favored examples are differential (Nomarski) interference contrast (DIC) (74) and phase contrast (PC) optics. Often, there is little or no color or transmission contrast between objects and background. There are, however, differences in refraction index, which give rise to a change in the optical path through the object, along with a change in the phase of the light passing through the object relative to that of the light passing through the surrounding medium. These phase differences can then be translated into visible intensity differences between the object and the background.

For the study of emulsions and the measurement of droplet size, high sophistication of the optics is not generally necessary. However, when droplets flocculate into complex structures, ordinary optics may not be able to provide a satisfactory clear image of the structure; DIC can much improve this. Figure 4 shows the three-dimensional (3-D) representation of the sample which DIC can provide.

It is natural at this point to define the factors limiting the applicability of VM. First, the sample must have certain optical properties, since the technique relies on the reflection, refraction, scattering, and absorption of radiation, for instance, visible light, as is the case for optical microscopy. For emulsions, this means that the sample must be transparent and that the continuous liquid and the droplets must have different refractive indices or different colors, i.e., properties which make them optically distinguishable. Second, the *resolution limit*, and hence the operational size domain, is governed by the wavelength of the illumination. This feature is known as the Rayleigh limit (75) [Eq. (1)] and results in a physical limit of about 0.2 μm (half the illumination wavelength) (76). The practical limit tends to be slightly higher, because of rapidly increasing measurement error with decreasing object dimensions (p. 47 in Ref. 77). This is caused by diffraction; the image of an object is actually a diffraction pattern, and the overlapping patterns of closely spaced objects result in image blurring. Regarding *magnification*, there is no theoretical upper limit. Still, increasing the magnification only renders larger, blurred images of the objects. Innovations in optics have, however, proven the diffraction-imposed barrier not to be absolute (78).

The Rayleigh criterion (75):

$$R = \frac{0.61\lambda}{N.A.} \tag{1}$$

where λ is the illumination wavelength, and *N.A.* is the numerical aperture.

VEM, and in particular when coupled with PC and DIC optics, permits some bending of the Rayleigh criterion. Jokela et al. (32) experienced a VEM resolution limit that was about half that stated by the criterion (0.1 urn). As described above, the absence of a magnification limit allows observation of objects smaller than the resolution limit, but the images will appear blurred with lack of detail. However, the contrast-enhancing ability of VEM, PC, and DIC can help clarify minute features normally lost owing to the blur-

ring diffraction patterns; e.g., Allen (79) observed the behavior of individual 25-nm diameter microtubules.

For VM, there is in addition the discretization of the image resulting from the digitization. The image is transformed into a matrix of colored or gray-scale dots, the pixels. The spatial dimensions of the pixels set the actual resolution of the image.

A further restriction relates to the three-dimensionality of the sample. The image is necessarily two-dimensional (2-D), although an increased depth of field (in the direction normal to the image plane) can provide information about a thicker optical section of the sample. For emulsions, this feature is clearly rather important, as these are very much 3-D and structurally dynamic as well. The choice of where to place the focal plane can strongly influence the data. For examining droplets and sampling a population for determination of the droplet size distribution (DSD), the simplest way will be to accumulate the droplets along a narrow focal plane. If the method of sample preparation (i.e., the container) provides a sample with a volume large enough in three dimensions for the droplets to move by gravity (e.g., microslides, see Sec. Ill), the droplets will ultimately accumulate along either the upper (ceiling) or the lower (floor) wall of the cell. Thermal movement may cause a size distribution function within the cream or sediment (55), as smaller droplets will diffuse more strongly than larger ones in a direction normal to the sediment plane. However, this need not be a factor, given large enough droplets or depth of field. It is more likely that small droplets will avoid measurement by not sedimenting into the focal plane within the time of measurement (Fig. 5). This exemplifies one of the clearer shortcomings of the technique - the 2-D representation of 3-D data.

Frequently, another restriction arises from the nature of the emulsion sample, namely that of disperse concentration. High droplet concentrations can cause droplet overlap, and small droplets tend to be obscured in strongly flocculating systems. Often, some degree of dilution is required, the chemical system allowing. As this may lead to changes in emulsion stability and consequently droplet size, it is important to apply dilution methods that do not influence the sample adversely in an uncontrolled manner. Basically, in surfactant-stabilized emulsions where the parameter of interest is dro-plet size, it may prove useful to dilute with the liquid of the continuous phase containing the surfactant at corresponding concentrations. This is, however, system dependent. For example, it usually proves sufficient to dilute crude oil-based W/O emulsions by adding the original crude oil. In any case, it is vital to control any changes in component concentrations which involve the crossing of phase boundaries and the distribution of components between phases. In creaming/ sedimenting emulsions the thickness of the cell will influence the degree of dilution necessary - a "thick" sample (long viewpath) represents a larger pool from which the droplet concentration at the chosen focal plane can increase.

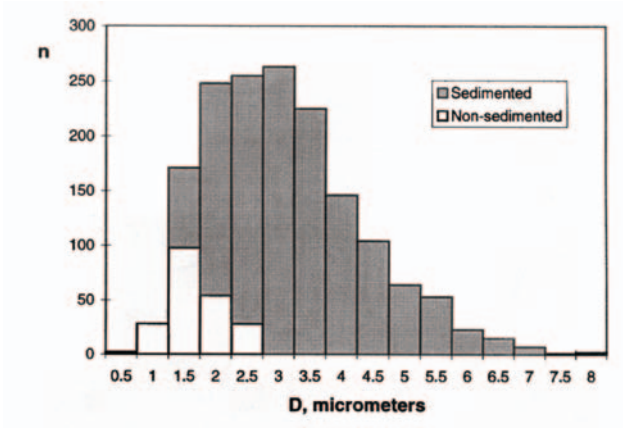

Figure 5 Effect of Brownian motion on the measurement of the DSD in a sediment. Small droplets take part in chaotic thermal motion in a direction normal to the sediment plane. The histogram shows that a significant part of the smaller droplets are withdrawn from the DSD as measured in the sediment; 67% of the droplets measured in the 1-μm class were not found within the sediment.

III. SAMPLE PREPARATION

Sample preparation is a science in itself, due to the diversity of the systems studied with microscopy. Emulsions can be prepared in several ways, according to which parameters one seeks to observe and measure. The most common way of studying a sample droplet deployed between an object slide and a cover slide is prone to pollution and distortion (evaporation, shear). Often, some form of sample cell may be used with advantage. Hollow, flat microcapillaries are one example (Fig. 6). Within such a cell, the sample can remain protected against the surrounding working environment, which makes them ideal for long-term observation.

A microslide is a flat, rectangular glass tube with plane-parallel cross-section. A liquid sample can be introduced simply by letting capillary forces pull the liquid into the slide. The prepared sample can then be secluded from the surroundings by covering the tube ends, e.g., with some

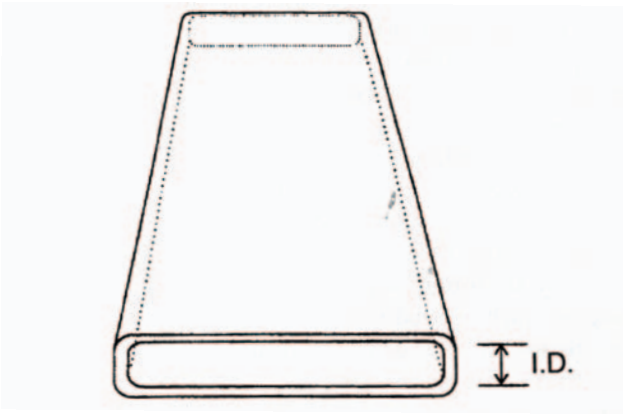

Figure 6 The microslide - a thin, flat rectangular micro-capillary of glass, useful for preparation of liquid samples vulnerable to evaporation or shear.

inert wax or grease. This way, the risk of evaporation and contamination altering the sample can be reduced significantly. However, the slide is made from glass and is therefore susceptible to influence from the sample. The surface is not perfectly smooth. Further, glass is slightly negatively charged, and will interact with other charged species in the sample, e.g., charged droplet surfaces. Adsorption at the interface by an anionic surfactant would expectedly reduce droplet/glass attraction, extending the lifetime of the sample and allowing observations of droplet kinetics over time.

Well-stabilized emulsions are not so vulnerable as to change through immediate coalescence. This fact can be utilized by letting droplets cream or sediment to the upper or lower cell wall, forming a slightly concentrated layer within a narrow focal zone. This simplifies the accumulation of data. However, if the droplets tend to coalesce rapidly upon collision, or it is desirable to retain the 3-D structure of the sample, one may increase the viscosity of the continuous phase (e.g., glycerin) or solidify the sample altogether (freezing). For kinetic studies, a cell preparation technique must be used (29, 30, 38, 41, 48, 54, 55).

Jokela et al. (32) developed a flowcell system for VEM-assisted DSD measurements. Images of nonsedi-mented droplets were analyzed, and the method per-formed favorably compared to light-scattering and Coulter-counting methods. It follows that such a technique would work better with less-stabilized droplets than would the microslide technique, as droplet contact (with each other or the cell walls) could be reduced. The central features of VEM-assisted DSD determination are discussed in Ref. 32.

Further, the properties of glass surfaces can be changed to suit the current experiment. A common procedure in, for example, chromatography, is silylation, which allows alteration of the surface hydrophilicity by introducing a less polar substituent at the silanol groups. An example of a silylating agent is HMDS (hexamethyldisilazane), which reacts with the glass by the following reaction (80):

$$(CH_3)_3Si - N - Si(CH_3)_3 + 2 - Si - OH \rightarrow 2 - Si - O - Si(CH_3)_3 + NH_3$$

The less polar and geometrically restricting -$Si(CH_3)_3$ now extends outwards from the surface, efficiently reducing surface polarity and also functioning as a steric repulsor. Other reagents can provide a range of properties, e.g., through different alkyl-substitutent chain lengths.

IV. IMAGE ENHANCEMENT

Image enhancement signifies any process, which when applied to the image, improves its quality, hereunder clarifying the features of interest for the subsequent analysis and measurements. Before the arrival of the digital age, simple but valuable enhancement operations were performed with the aid of specialized equipment. Now, image-enhancement software permits the same and more to be done digitally, increasing method versatility tremendously. The different processes vary greatly in complexity and, hence, the computational power required. However, currently available computers provide this in affluence at minimal cost, leaving the main issue to be the flexibility of the software (often three times as expensive as the machinery on which it is run).

The first category of enhancement processes work on every pixel, disregarding its immediate neighborhood. Typically, this encompasses enhancement of contrast and adjustment of brightness. These functions have been available since before the introduction of the computer into the microscopy setup, through analog image enhancers (made obsolete through digital treatment of the image). Seemingly trivial, a little effort here can greatly contribute to the quality of the data to be extracted at a later stage, as well as making the task easier. The second class of procedures works on each pixel relative to the adjacent pixels. Typically, a matrix assigning new values to the central pixel and its neighbors, altering their relative intensities, is run across the image. This is used for enhancing edges, filtering out noise, etc., and represents a very powerful way in which to

improve image quality. Figure 7 shows how blur and noise can be removed, enhancing detail and preparing the image for analysis.

V. IMAGE ANALYSIS AND MEASUREMENT

An image contains a lot of information that in different ways can be useful when attempting to describe the sample. However, when the task at hand is that of determining droplet size and the size distribution, the procedure of measurement uses only a small amount of this information. In its purest sense, the procedure seeks to distinguish the droplets from their surround-ings (the background) and from each other, and then to perform the measurement on each of the defined droplets. The most primitive way is, of course, when the operator performs both the denning and measurements manually, a course which does not really need the assistance of a computer (although this may somewhat ease the tedious work). For complex systems this may be the only way to go, because the decision process of defining separate droplets is too complicated for a practical and reliable use of automated procedures that may be found within the software. For simpler systems, such procedures may tremendously simplify the generation of statistically sufficient amounts of reliable data, making the method a competitive alternative. Readily analyzable samples are typically dilute and nonflocculated, with a rather narrow distribution of droplet sizes. Figure 8 shows an image which does not permit automated measurement.

The general procedure is simple: first, define the parameters distinguishing the droplets from the back-ground. This is typically accomplished by performing a thresholding on the basis of gray scale (or color) pixel values characteristic to the droplets. The second step is based on shape criteria; a droplet has a monotonic curvature, and a break in the monotony represents a droplet-droplet contact. The images in Fig. 9 show the analysis and measurement procedure. The resulting histogram is shown in Fig. 9e.

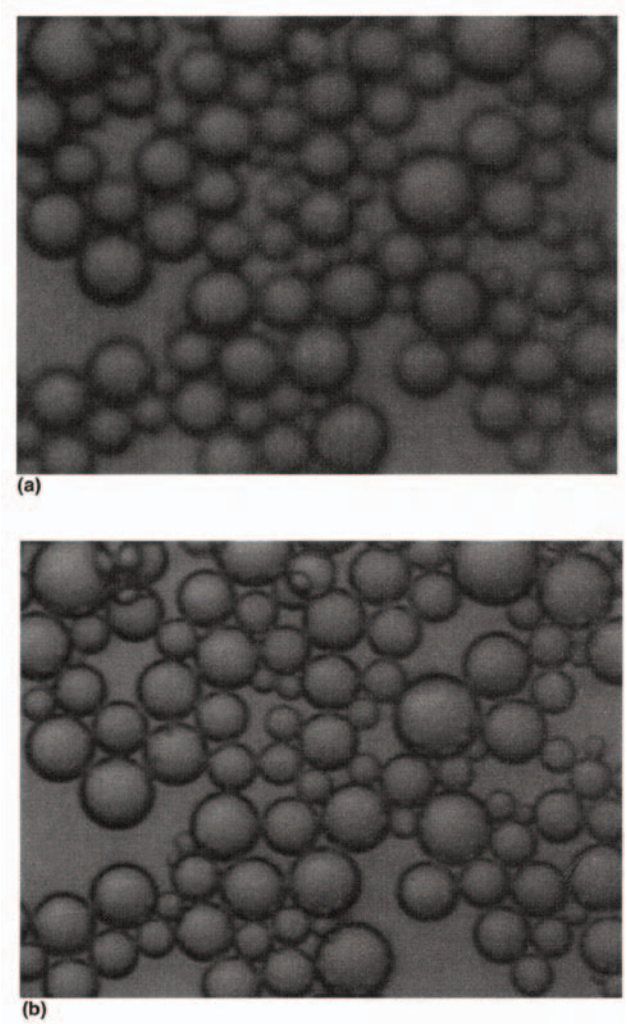

Figure 7 Sharpening of image features: before (a) and after (b) spatial filtering.

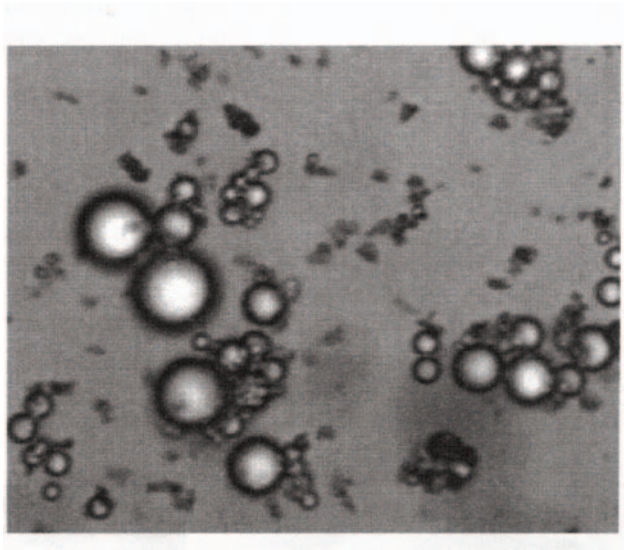

Figure 8 Analytically demanding emulsion: droplets are largely coagulated into 3-D floes; particles are present in the droplet size range. Such an image is extremely hard to analyze by automated software routines, and consequently demands strong participation by the operator. On the other hand, this procedure remains the only true alternative for handling such systems, as other techniques will not be able to resolve flocs or even discriminate between particles and droplets.

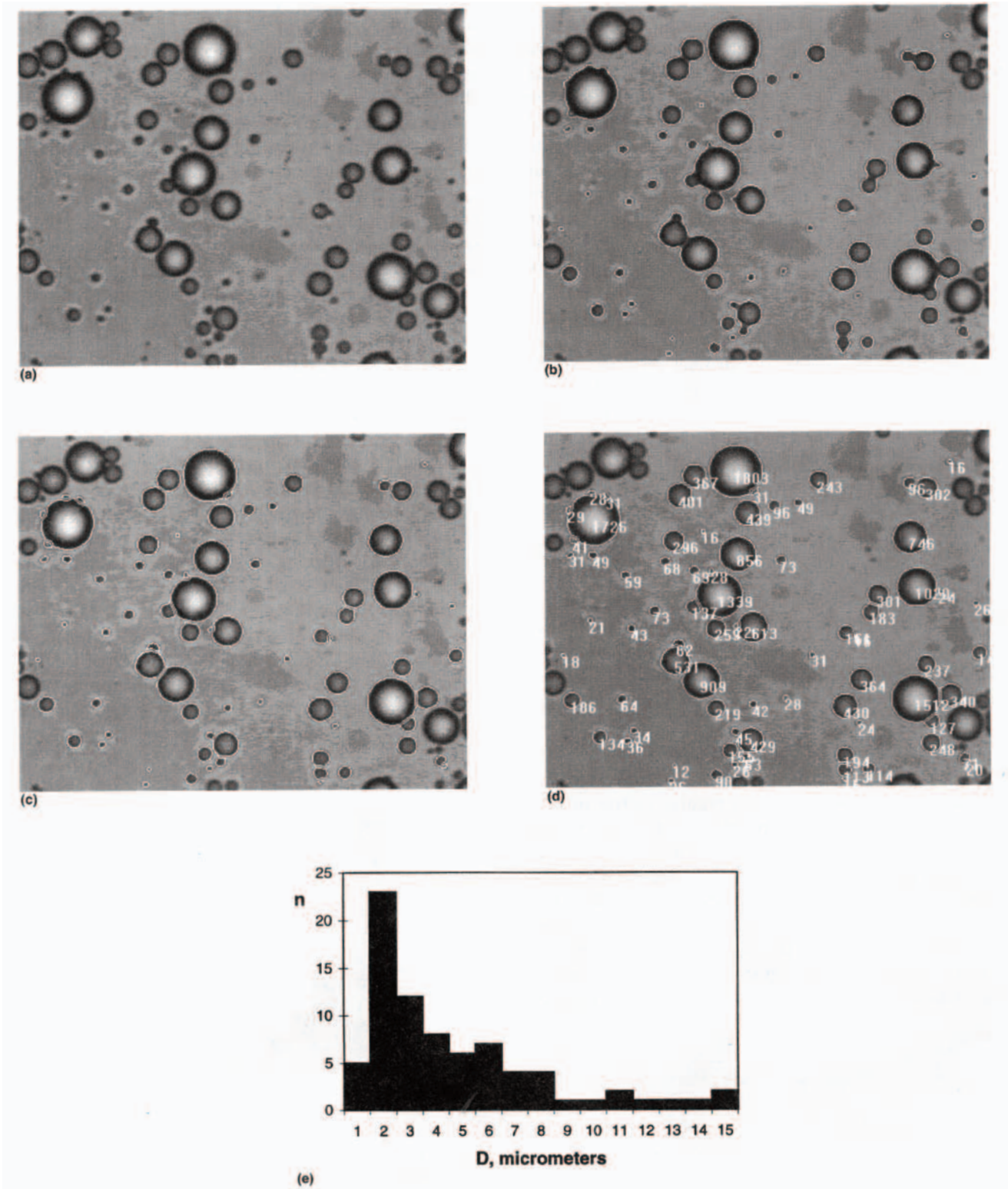

Figure 9 A readily analyzable image; droplets are clearly distinguished from the background by characteristic gray-tone values, and flocs are 2-D: (a) the raw image; (b) thresholding - defining droplet pixel values; (c) separating droplets within floes; (d) measurement of resolved image; (e) DSD of image.

When measuring the droplet size manually, the diameter comes out directly. The automated procedure will attempt to calculate the diameter from the droplet outline resulting from the thresholding. If, for some reason, the droplet is distorted and has an ellipsoidal shape, the return value might be the maximum, the minimum, or an average value, according to the set preferences. It may instead prove useful to measure the area within the outline and calculate the diameter on the basis of this. In any event, it is crucial to be aware of the criteria on which the program founds its return values.

Figure 10 serves as an example of calculation of the droplet diameter from the area of the pixel disk that was denned as belonging to a droplet through thresholding (Waddel disk diameter, D_{WD}). The pixel dimen-sion is 0.23 μm, giving a pixel area of 0.0529 μm^2. The number of pixels in the 1-μm diameter disk is 16, while 61 pixels give 2 μm, and 132 pixels give 3 μm. Equation (2) yields the D_{WD}

$$D_{WD} = \left(\frac{A_p n_p}{\pi}\right)^{\frac{1}{2}} \cdot 2 \qquad (2)$$

where A_p is the area of each pixel, and n_p is the number of pixels in the disk. From the Fig. 10 it is clear that the potential error accompanying the D_{DW} increases rapidly with decreasing droplet (disk) size.

VI. TREATMENT OF VM SIZE DATA

The digital image consists of a regular matrix of pixels, which means that the number of different values that can be measured is limited. In reality, of course, the distribution is continuous; the digitization imposes discretization. In any case, since this is a direct method and the number of droplets counted and measured is finite, the resulting distribution will take the shape of a histogram. The histogram shows the frequency distribution for the assigned number and width of classes. A higher number will, when applied to a sufficiently high number of measurements, give a better representation of the overall shape of the real population distribution.

It is suggested (81, 82) that the class width should be chosen according to the distribution width; arithmetic progression (width constant, independent of droplet size) is sufficient for narrow distributions, while broad distributions should be presented with progressively increasing class width with increasing droplet size (equal differences between logarithms of the diameters, geometric progression). The reason for this is the fact that emulsion droplet diameters tend to be lognormally distributed (81, 83, 84).

The frequency distribution of diameters is the most widely used way of presenting population size data. It contains useful information which aids the prediction of emulsion kinetic behavior; e.g., sedimentation and diffusion are functions of droplet size. Also, one can follow the evolution of the DSD as a function of time, the shift towards fewer/larger droplets being evidence of droplet-depletion mechanisms, such as coalescence and Ostwald ripening. From the distribution, the kinetic coefficients can be calculated, allowing prediction of how the DSD will develop (e.g., 48, 55). This is described in detail by Dukhin et al., Chapter 4, this volume. Figure 11 shows how the addition of a demulsifier can destabilize an emulsion and bring about emulsion resolution. The example is a water-in-crude oil emulsion, the demulsifier a phenolic resin alkoxy-late.

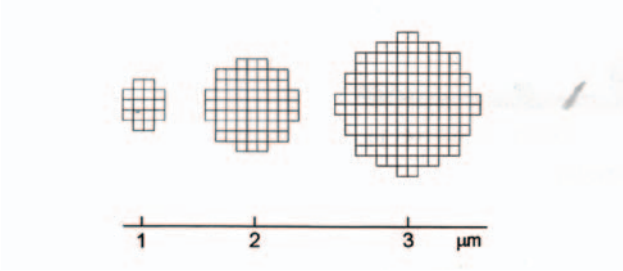

Figure 10 Influence of digital resolution on the exactness of measurements.

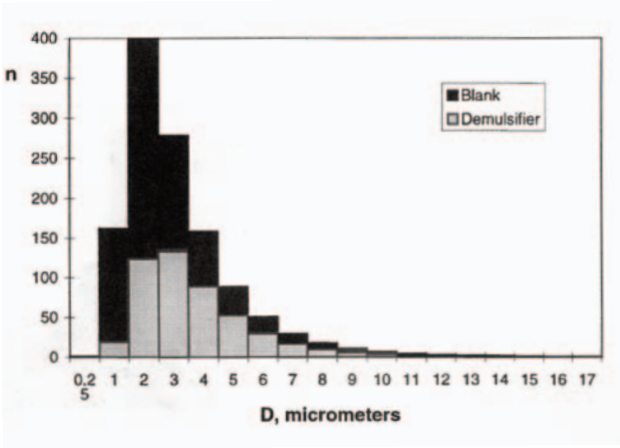

Figure 11 Effect of a demulsifier; a phenolic resin alkoxylate commercial demulsifier accelerates water/crude oil resolution. The demulsifier was added to 50 ppm to a 40% (v/v) water/oil [7.8 wt% asphaltene in 30/70 (v/v) toluene/decane]. The histogram shows the DSDs of the emulsion with demulsifier and the reference emulsion after about 2 h.

It is often more useful to apply cumulative distribu-tions to illuminate characteristic features of and difference between datasets. The cumulative distribution adds the contents of the next class to the sum of all previous classes, yielding the well-known S-curve for normal or lognormal distributions. Figure 12 shows the normalized cumulative volumes of four emulsions with varying contents of surface-active matter. Asphaltenes and resins are classes of large, surface-active molecules found in crude oil. These are expected to be responsible for the stabilization of water droplets mixed into the oil, and the relative amounts and properties of asphaltenes and resins present in the oil will affect their state and emulsifying behavior. Figure 12 shows how the introduction of a resinous fraction may improve the emulsifying power of an asphaltene surfactant fraction. All emulsions were prepared as a 40% (v/v) solution of 3.5% NaCl in a 70/30 (v/v) decane/ toluene oil with asphaltene/resin. The asphaltene fraction was the pentane-insoluble part of a crude oil, while the resin fraction was adsorbed from the pentane eluate on to silica, then washed with benzene and desorbed with a methanol/dichlorodecane mixture. As can be seen in Fig. 12, a "high" asphaltene content (1.5 wt% of the dispersed phase) can stabilize a larger interfacial area than a "low" concentration (0.5 wt%), putting a greater part of the dispersed volume in small droplets. The "low" asphaltene content emulsion also shows that a great part of the dispersed volume is found within a few large droplets, reducing the accuracy of the DSD determination. Introducing a resinous fraction, a "low" concentration (6.31% the mass of asphaltene) has little effect on the relative distribution of droplet sizes within the two emulsions, while a "high" concentration (25%) further increases the emulsifying power of the asphaltene fraction, resulting in a still higher part of the dispersed volume to be found amongst small droplets. It has been suggested (85) that resins may assist the inclusion of asphaltene aggregates into the water/oil interface, thus improving its stabilization. A 70/30 (v/v) decane/toluene oil contains both monomeric and aggregated asphaltene; aromatic toluene is a good asphaltene solvent, while decane is not.

Measurement of small droplets is more prone to error than measurements of large (though undistorted, see below) droplets. However, given a 1-μm class width and 10% error in the diameter of a 2-μm droplet [D □ (1.8-2.2 μm)], the measurement will still be recognized in the histogram as an element in the 2-μm class. In a common VEM set-up with a 60 × magnification microscope objective a typical digital resolution is of the order 0.1 μm/pixel. A 10% measurement error for a 1-um droplet is then the equivalent of 1 pixel, 2 pixels for a 2-μm droplet, and so on. As a consequence of this, it is clear that the relative error of a measurement decreases with increasing droplet size. Figure 13 shows the problem of approaching the digital resolution limit.

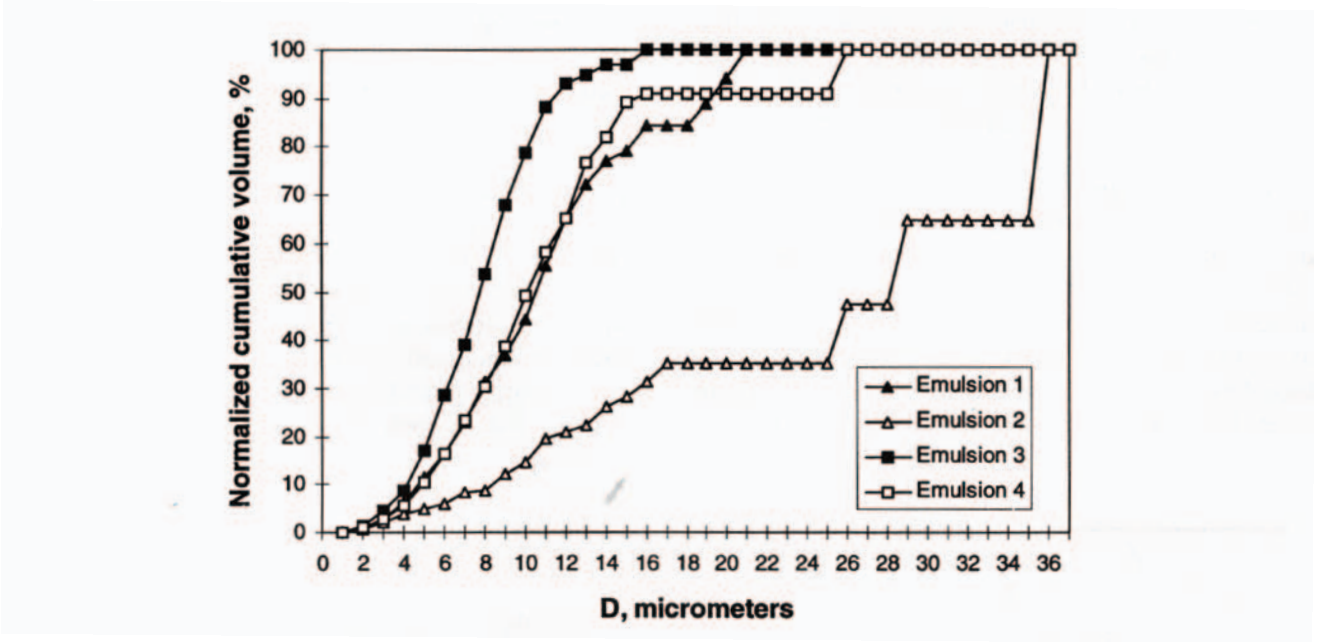

Figure 12 Water droplets in model oils with asphaltene and resin fractions extracted from a crude oil; normalized cumulative volume showing the effect of asphaltene and resin content. Key: emulsion 1 - high asphaltene, no resin; 2 - low asph., no resin; 3 - high asph., high resin; 4 - high asph., low resin.

Figure 13 Example of decreasing reliability of measurement of small droplets when approaching the digital resolution of the image (example: 0.2326 μm/pixel): 1 pixel renders a Waddle disk diameter of 0.25 μm; 4 pixels - 0.5 μm; 8 pixels - 0.75 μm. All objects will register within the 0.5-μm class (given 0.5-μm width.)

As droplets grow larger, gravity can affect their shape. This is also a function of interfacial tension -higher interfacial tension acts to uphold the spherical shape. This means that there is an upper limit above which measurements will be increasingly marred by error. When observing droplets residing on the cell wall in a direction parallel to the direction of gravity, which is normally the case, the droplets will appear to be circular, but the diameter of the oblate will be larger than that of the volume-equivalent sphere, as illustrated in Fig. 14.

Often the brightness levels characterizing the droplet outline may vary with droplet size. This can influence the thresholding process, where the outer boundaries of the droplets may be wrongly set, causing underestimation of the size. Again, this underlines the importance of proper image preprocessing prior to analysis.

Due to the directness of the VM method, the exactness of the single measurements should be high. However, to describe the true shape of the population profile a high number of measurements is needed for statistical reliability. To achieve an error of 5% at the 95% confidence level, 740 droplets must be counted (86).

Different representations of the data will be differently influenced by missing data, which is, typically, an undercounting of droplets within the extreme size classes of the population. When using a mass- or volume-based distribution, an underestimation of dro-plets at the upper end of the size scale may severely reduce the correctness of the distribution, as one 20-μm droplet has the mass and volume of 1000 2-μm droplets. It is easily realizable that if 1000 droplets are counted from, say, three or four images, the num-ber of large droplets counted may not be truly representative of the sample. This will cause a shift in the distribution. However, it is to some extent possible to perform a mathematical fit of the data set (when key features of the distribution function are known), thus reducing the adverse influence of missing data. Such a fit is shown in Fig. 15.

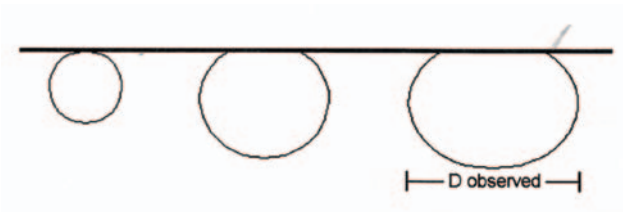

Figure 14 Gravity-induced deformation of droplets.

VII. SUMMARY

The use of microscopy for emulsion studies is well established and the technique is generally regarded as a reliable way of generating, for example, DSDs. Traditionally, a labor demanding and tedious task, emerging image-analysis software technology provides opportunities for automated or partially automated droplet counting and measurement. However, alterna-tive methods are often favored owing to a higher degree of simplicity of operation (which in parallel makes them quicker). Still, microscopy remains the only technique that offers direct observation of the sample, a feature that allows a greater control of sample state - e.g., degree of flocculation - which is unri-valled by any other technique. Another important advantage is the ability to follow the behavior of single droplets or a set of droplets, which creates opportunities for studies of droplet-droplet interactions. The examples included in the chapter attempt to underline the sensitivity and versatility of derived methods. Through developments in the fields of optics and image enhancement and analysis, VM will find conti-nuingly expanding applicability within very diverse research disciplines.

ACKNOWLEDGMENTS

The technology program Flucha, financed by The Norwegian Research Council (NFR) and the oil industry, is ac-

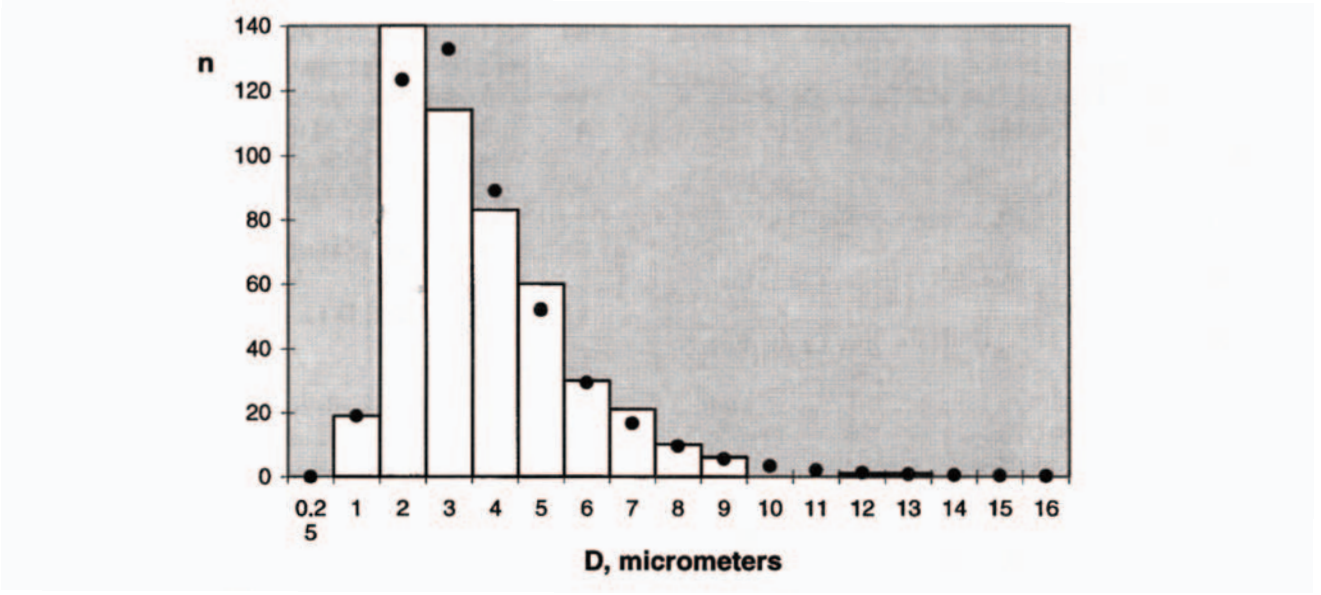

Figure 15 Curve fitting of data to a lognormal distribution function.

knowledged for a PhD grant and financial support.

REFERENCES

1. S Bradbury. Microsc Anal (May): 7—12, 1990.
2. P Walstra, H. Oortwijn. J Colloid Interface Sci 29: 424—431, 1969.
3. A Takamura, S Noro, S Ando, M Koishi. Chem Pharm Bull 25: 2644—2649, 1977.
4. J Drelich, G Bryll, J Kapcynski, J Hupka, JD Miller, FV Hanson. Fuel Process Technol 31: 105—113, 1992.
5. K Eberth, J Merry. Int J Pharm 14: 349—353, 1983.
6. O Flint. Microsc Anal (March): 19—23, 1991.
7. RA Mohammed, AI Bailey, PF Luckham, SE Taylor. Colloids Surfaces 83: 261—271, 1994.
8. C Orr. In: P Becher, ed. Encyclopedia of Emulsion Technology. Vol 3. New York: Marcel Dekker, 137—169, 1988.
9. A Takamura, S Noro, S Ando, M Koishi. Chem Pharm Bull 25: 2617—2623, 1977.
10. RH Muller, S Heinemann. Clin Nutr 11: 223—236, 1992.
11. T Kubo, S Tsukiyama, A Takamura, I Takashime. Yakugaku Zasshi (Japan) 91: 518—521, 1971.
12. SK Mason, K May, S Hartland. Colloids Surfaces 96: 85—92, 1995.
13. C-J Lee, S-S Wang, C-C Chan. J Chin Inst Chem Eng 26: 263—275, 1995.
14. A Bhardwaj, S Hartland. J Disp Sci Technol 15: 133—146, 1994.
15. EE Isaacs, H Huang, AJ Babchin, RS Chow. Colloids Surfaces 46: 177—192, 1990.
16. M Sato. IEEE Trans Ind Applic 27: 316—322, 1991.
17. M Deitel, KL Friedman, S Cunnane, PJ Lea, A Chaiet, J Chong, B. Almeida. J Am Coll Nutr 11: 5—10, 1992.
18. FD Rumscheidt, SG Mason. J Colloid Sci 16: 238—261, 1965.
19. RD Hamill, RV Petersen. J Pharm Sci 55: 1268—1274, 1966.
20. RD Steele, JE Halligan. Sep Sci 9: 299, 1974, 299—311, 1974.
21. DD Eley, MJ Hey, JD Symonds. Colloids Surfaces 32: 87—101, 1988.
22. Y Otsubo, RK Prud'homme. Rheol Acta 33: 303—306, 1994.
23. M Zerfa, BW Brooks. Chem Eng Sci 51: 3591—3611, 1996.
24. N Garti. Colloids Surfaces 123/124: 233—246, 1997.
25. R Pal. AIChE J 42: 3181—3190, 1996.
26. PJ Hailing. CRC Crit Rev Food Sci Nutr 15: 155—203, 1981.
27. M Britten, HJ Giroux. J Food Sci 56: 792—795, 1991.
28. GH Hanna, KM Larson. Ind Eng Chem Prod Res Dev 24: 269—274, 1985.
29. ∅ Saether, SS Dukhin, J Sjöblom, ∅ Holt. Colloid J 57: 793—799, 1995.
30. ∅ Holt, ∅ Söther, J Sjöblom, SS Dukhin, NA Mishchuk. Colloids Surfaces 141: 269—278, 1998.
31. B Balinov, O Urdahl, O Söderman, J Sjöblom. Colloids Surfaces 82: 173—181, 1994.
32. P Jokela, PDI Fletcher, R Aveyard, JR Lu. J Colloid Interface Sci 134: 417—426, 1990.

33. I Fourel, JP Guillement, D Lebotlan. J Colloid Interface Sci 169: 119—124, 1995.
34. C Solans, R Pons, S Zhu, HT Davis, DF Evans, K Nakamura, H Kunieda. Langmuir 9: 1479—1482, 1993.
35. AW Pacek, IPT Moore, RV Calabrese, AW Nienow. Trans Inst Chem Eng A: Chem Eng Res Des 71: 340—341, 1993.
36. AW Pacek, AW Nienow, IPT Moore. Chem Eng Sci 49: 3485—3498, 1994.
37. AW Pacek, AW Nienow. Trans Inst Chem Eng A: Chem Eng Res Des 73: 512—518, 1995.
38. NA Mishchuk, SV Verbich, SS Dukhin, ∅ Holt, J Sjöblom. J Disp Sci Technol 18: 517—537, 1997.
39. TC Scott, WG Sisson. Sep Sci Technol 23: 1541—1550, 1988.
40. AW Pacek, IPT Moore, AW Nienow, RV Calabrese. AIChE J 40: 1940—1949, 1994.
41. ∅ Holt, ∅ Ssther, J Sjöblom, SS Dukhin, NA Mishchuk. Colloids Surfaces 123/124: 195—207, 1997.
42. SI Pather, SH Neau, S Pather. J Pharm Biomed Anal 13: 1283—1289, 1995.
43. AH Kamel, SA Akashah, FA Leeri, MA Fahim. Comput Chem Eng 11: 435—139, 1987.
44. RD Hazlett, RS Schechter, JK Aggarwal. Ind Eng Chem Fundam 24: 101—105, 1985.
45. B Balinov, O Söderman, T Warnheim. J Am Oil Chem Soc71: 513—518, 1994.
46. X Li, JC Cox, RW Flumerfelt. AIChE J 38: 1671—1674, 1992.
47. Y Wang, S Bian, D Wu. Pestic Sci 44: 201—203, 1995.
48. ∅ Söther, J Sjöblom, SV Verbich, NA Mishchuk, SS Dukhin. Colloids Surfaces 142: 189—200, 1998.
49. UT Lashmar, JP Richardson, A Erbod. Int J Pharm 125: 315—325, 1995.
50. WL Lammers, HJ van der Stege, P Walstra. Neth Milk Dairy J 41: 147—160, 1987.
51. B Kachar, DF Evans, BW Ninham. J Colloid Interface Sci 100: 287—301, 1984.
52. K Florine-Casteel. Biophys J 57: 1199—1215, 1990.
53. JC Crocker, DG Grier. J Colloid Interface Sci 179: 298—310, 1996.
54. ∅ Holt, ∅ Söther, J Sjöblom, SS Dukhin, NA Mishchuk. Colloids Surfaces 141: 269—278, 1998.
55. ∅ Ssther, J Sjöblom, SV Verbich, SS Dukhin. J Disp Sci Technol 20: 295—314, 1999.
56. SV Verbich, SS Dukhin, A Tarovski, ∅ Holt, ∅ Söther, J Sjöblom. Colloids Surfaces 123/124: 209—223, 1997.
57. H Matsumura, K Watanabe, K Furusawa. Colloids Surfaces 98: 175—184, 1995.
58. PT Spicer, W Keller, SE Pratsinis. J Colloid Interface Sci 184: 112—122, 1996.
59. SR Deshiikan, KD Papadopoulos. J Colloid Interface Sci 174: 302—312, 1995.
60. W Bartok, SG Mason. J Colloid Sci 14: 13—26, 1959.
61. J Bongers, H Manteufel, K Vondermassen, H Versmold. Colloids Surfaces 142: 381—385, 1998.
62. JC Crocker, DG Grier. Phys Rev Lett 73: 352—355, 1994.
63. A Bhardwaj, S Hartland. Ind Eng Chem Res 33: 1271—1279, 1994.
64. KL Alexander, D Li. Colloids Surfaces 106: 191—202, 1996.
65. P Cheng, D Li, L. Boruvka, Y Rotenberg, AW Neumann. Colloids Surfaces 43: 151—167, 1990.
66. D Li. Colloids Surfaces 116: 1—23, 1996.
67. SS Susnar, HA Hamza, AW Neumann. Colloids Surfaces 89: 169—180, 1994.
68. DY Kwok, P Chiefalo, B Khorshiddoust, S Lahooti. ACS Symp Ser 615: 374—386, 1995.
69. SE Taylor. Colloids Surfaces 29: 29—51, 1988.
70. R. Isherwood, BR Jennings, M Stankiewicz. Chem Eng Sci 42: 913—914, 1987.
71. H Førdedal, E Nodland, J Sjöblom, OM Kvalheim. J Colloid Interface Sci 173: 396^05, 1995.
72. H Førdedal, Y Schildberg, J Sjöblom, J-L Voile. Colloids Surfaces 106: 33—47, 1996.
73. H Kallevik, OM Kvalheim, J Sjöblom. J Colloid Interface Sci 225: 494—504, 2000.
74. RD Allen, GB David, G Nomarski. Z Wiss Mikrosk 69: 193, 1969.
75. M Spencer. Fundamentals of Light Microscopy. New York: Cambridge University Press, 1982.
76. EM Chamot. Elementary Chemical Microscopy. New York: John Wiley, 1915.
77. DJ Shaw. Introduction to Colloid and Surface Chem-istry. 4th ed. Oxford: Butterworth-Heinemann, 1991.
78. PM Cooke. Analyt Chem 64: R219-R243, 1992.
79. RD Allen. Annu Rev Biophys Chem 14: 265, 1985.
80. T Takei, A Yamazaki, T Watanabe, M Chikazawa. J Colloid Interface Sci 188: 409—14, 1997.
81. C Orr. In: P Becher, ed. Encyclopedia of Emulsion Technology. Vol 1. New York: Marcel Dekker, 369—404, 1983.
82. T Allen. Particle Size Measurement. 2nd ed. London: Chapman & Hall, 1974.
83. I Bajsic, B Blagojevic. Strojniski Vestnik [Mech Eng J] 36: E1—E8, 1990.
84. HHG Jellinek. J Soc Chem Ind 69: 225, 1950.
85. JD MacLean, PK Kilpatrick. J Colloid Interface Sci 196: 23—34, 1997.
86. WJ Dixon, FJ Massey Jr. Introduction to Statistical Analysis. 3rd ed. New York: McGraw-Hill, 1969, p550.